FRACTOGRAPHY AND THE SHAPE OF PART-THROUGH CRACKS

M. Prodan*, J.C. Radon**

Crack growth through highly varying stress fields favors the formation of part-through surface cracks. Earlier studies were concerned with macroscopic problems of fracture mechanics, more recently our attention was directed towards microscopic (SEM) investigations. The central and deepest part of the surface crack front seems to respond in a predictable way to stress intensity factors, governed by conditions of local plane strain; this behaviour is described in detail.

INTRODUCTION

The evaluation of the stress intensity factor K along the crack front of a part-through crack is a complex 3D problem. However, the Finite Element (FE) results such as those of Raju and Newman (1) have been shown to be quite useful for the analysis of the fatigue growth of surface cracks. A computational procedure was developed by Prodan (2), which calculates the cyclic stress intensity factor ΔK_i for a series of crack depths a_i of a growing part-through crack. Using the Finite Element Boundary Correction Factor (1), it then fits the CT specimen formula to these data, i.e. it determines experimental parameters that reproduce an equivalent growth of ΔK with crack depth (length) "a" in a tensile plate and corresponding CT specimen.

The main topic of this paper is the scanning electron microscope (SEM) examination of the fracture surface and the determination of the shape and size of part-through fatigue cracks.

* Swiss Federal Institute for Reactor Research, Würenlingen, CH
** Imperial College, London, U.K.

FRACTOGRAPHY

Figure 1 shows macroscopic fractographic records of two specimens. The initial geometries of all seven tested plate specimens were similar in that they contained a starter notch $a_0 = 2$ mm and $2c_0 = 14$ mm growing under identical testing conditions (see also Fig. 3). The fatigue crack growth behaviour could be reproduced with the plate specimens to a high degree of accuracy.

A typical micrograph (SEM) is shown in Fig. 2. The piece was taken from the centre of the specimen $a \approx 16$ mm, $\Delta K \approx 1250$ N mm$^{-3/2}$. The material used was a fine-grain structural steel BH 43 W (or St. E. 43). For the mechanical properties and chemical analysis of the steel, see the relevant German Standard (St. E. - W' blatt 089). Figure 2 shows a detail in the region of the marking line on the fracture surface of one of the tensile plates. A faint marking line, visible to the naked eye, on the second test piece, Fig. 1, was produced by a load changing technique. The investigated region, Fig. 2, was chosen from the centre of the specimen typically plane strain conditions but did not show significant difference from the surface of the plate which clearly is in plane stress conditions (also investigated but not illustrated in this paper). The fracture surface is a record of the loading experienced by the specimen or the structure in service. Certain features of the loading can be observed on the macroscopic scale. This is particularly true at longer crack lengths. Higher loads produce a rougher surface which appears darker (see the surface of the final static fracture in Fig. 1), while lower loads produce a much smoother and brighter surface (see fatigue part of the fracture surface in Fig. 1). From the micrograph, Fig. 2, a fine-grain fatigue fracture surface structure can be established. The assumptions of homogeneity and isotropy, necessary for the application of fracture mechanics methods, were shown to be valid in this case. No attempt was made to obtain cyclic crack propagation rates through striation counting and measurement of spacings between them. In this context and under suitable conditions striations may be considered to represent successive positions of the crack front. However in the present tests striations would not be easy to investigate at constant amplitude loading, because of the multidimensional crack configuration. The single marking line according to a load increase ($\sigma_{Markmax} = 1,25\ \sigma_{max}$, $\sigma_{Markmin} = 0,9\sigma_{max}$ or $R_{Mark} = \sigma_{Markmin}/\sigma_{Markmax} = 0,7$; $N \approx 4000$ cycles) shows a region densely populated with microcracks, Fig. 2

CRACK SHAPES AND SIZES

In Fig. 3 CT specimens were adjusted to the part-through crack configuration in order to make the relation between the stress intensity factor and the crack length (depth) the same in both problems. This may be done approximately by selecting specific dimensions and loads of the CT specimen. The ΔK values of the growing part-through crack were calculated according to the Finite Element results (1) mentioned earlier; those of the crack in the CT specimen with correlated dimensions and loading according to (2) and the equation in ASTM E 399-81.

After the evaluation of the fatigue tests, the local crack advance was compared with the local stress intensity factor at the deepest point of the part-through crack front. As far as the evaluation of the crack shape was concerned, a good agreement was obtained with the local Paris law using growth rates measured on CT specimens. However the comparison of the cycle numbers of tensile plate and corresponding CT specimen experiments under identical testing conditions (except for the geometry) seemed not to be in agreement with the above model. This discrepancy may be explained in various ways, such as the inadequate fracture mechanics theory or incomplete fatigue crack growth laws, inadequate control of experimental conditions (e.g. insufficient elimination of the undesirable bending effects under uniform tension loading of the plates), etc. but these are all beyond the scope of this paper. Figure 4 summarizes observations of non-self-similar growth of part-through cracks according to Prantl et al. (3). A postulation in ASME Boiler and Pressure Vessel Code, Section XI, suggests that eventual crack growth shall be assumed to take place maintaining the a/c ratio of the original flaw. Figure 4 shows schematically that this assumption may be sometimes very incorrect (depending on the crack depth-to-length ratio) and consequently the distance in time and size between a real crack and the final critical crack overestimated. One of the problems lies in the fact that the propagation of the part-through cracks in the direction of the depth "a" cannot be measured directly since such a propagation cannot be easily recorded. A new crack measurement system using a Crack Microgauge for measuring surface cracks based on A.C. potential technique was introduced recently. The error in these measurements was generally less than ± 0,5 mm. New advances in the understanding of alternating current (A.C.) fields measurements, have resulted in the production of an improved instrument for crack measurement, the Crack Microgauge (manufactured by the Unit Inspection Company). With this instrument it is now possible to detect and measure relatively accurately surface cracks in any metal component or structure. The instrument is simple to operate, requires no formal instruction and needs no prior calibration with test blocks. Several applications and the theoretical background are described elsewhere (Dover and Collins (4), Musuva and Radon (5)).

Figure 5 presents a scanning micrograph of a CT specimen fatigue fracture surface. The piece was taken again from a region $a-a_0 \approx$ 16 mm, $\Delta K \approx 1200$ N $mm^{-3/2}$. Figures 5 and 2 show a good agreement in the relief and microstructure of the fracture surfaces. This is an important observation which supports the applicability of the mechanical-mathematical adjustment of the CT specimen to the plate.

DISCUSSION

The accepted methods for predicting failure conditions in engineering structures are mostly based on comparatively simple models, such as linear elastic fracture mechanics and simple rules for fatigue crack growth. A basic weakness of existing predictive methods is that they are not generally based on the understanding of fracture mechanisms likely to occur in service. It is the aim of the underlying fracture research to extend this knowledge, especially for correlating the microscopic fractographic observations with the macroscopic crack growth.

CONCLUSIONS

It was shown that the ΔK values of a part-through crack may be conveniently compared with those of a CT specimen. Micrographs of a surface crack and a crack growing in mode I in a CT specimen show a very similar fracture surface. This provides a further support for the applicability of the mechanical-mathematical adjustment of CT and surface crack geometries recently proposed.

ACKNOWLEDGEMENT

The authors wish to thank W. Muster and Mrs. J. Woodtli, EMPA Dübendorf (CH) for the SEM investigations.

SYMBOLS & ABBREVIATIONS

a, a_i	depth of part-through surface crack (plate) length of through-thickness crack (CT specimen)
c	half length of part-through surface crack (plate)
ΔF	cyclic load (force)
K	stress intensity factor
ΔK, ΔK_i	cyclic stress intensity factor
t	thickness
W	width
η	load per unit thickness of the CT specimen
$\Delta\sigma$	cyclic stress
ASME	American Society of Mechanical Engineers
CT	compact tension, acc. to ASTM E 399
3D	three-dimensional
LEFM	linear elastic fracture mechanics
SEM	scanning electron microscope

REFERENCES

1. Raju, I.S. and Newman, J.C., 1979, Engng. Fracture Mechanics, 11, 817
2. Prodan, M., 1981, Material und Technik (Zürich), 9, 29
3. Prantl, G., Varga, T. and Njo, D.H., 1978, Proc. IAEA-SM-218/3, Vol. II, 53
4. Dover, W.D. and Collins, R., 1980, British Journal of NDT, 22, 291
5. Musuva, J.K. and Radon, J.C., 1981, Proc. FATIGUE 81, IPC, SEE, p. 106

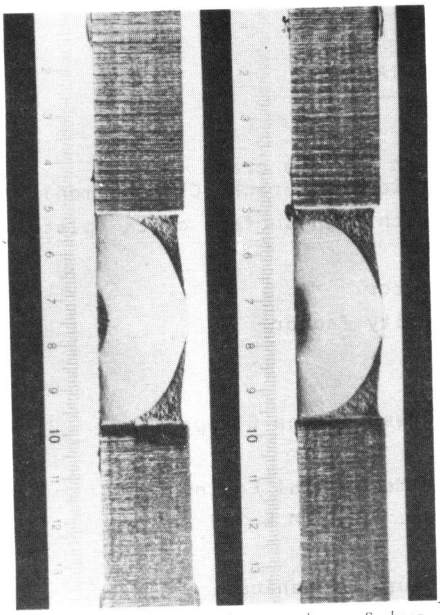

Fig. 1 Macrofractographs of two tensile plate specimens

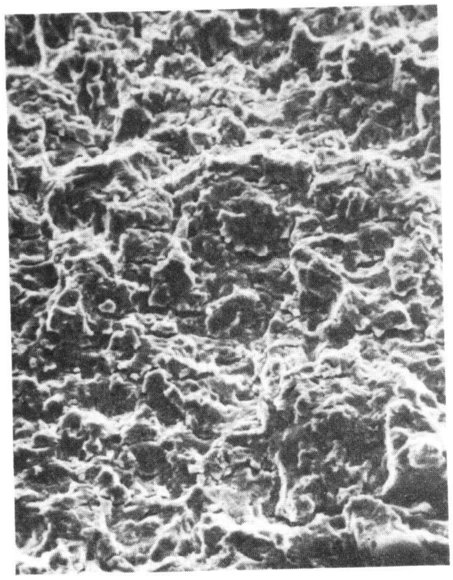

Fig. 2 Microfractograph in the centre of the specimen, a≈16 mm (500x magnification)

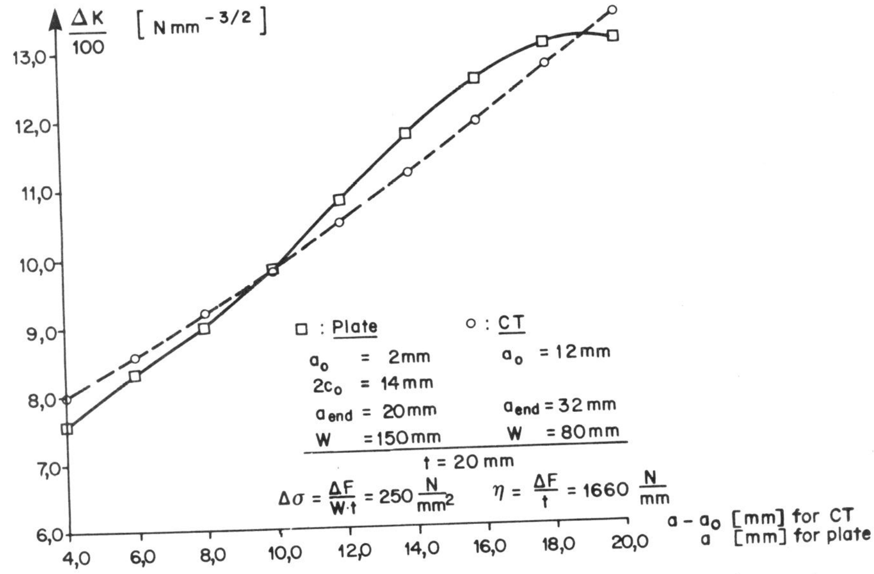

Fig. 3 Calculated K values of the growing part-through crack at the deepest point (middle) and of an adjusted CT specimen

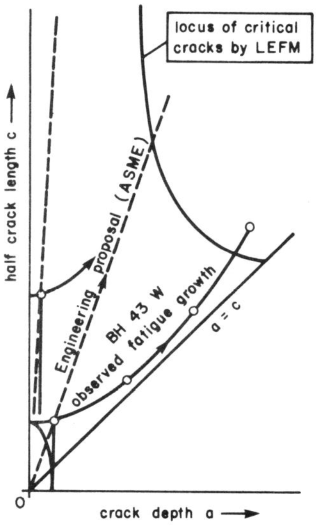

Fig. 4 Fatigue growth of surface cracks towards critical size

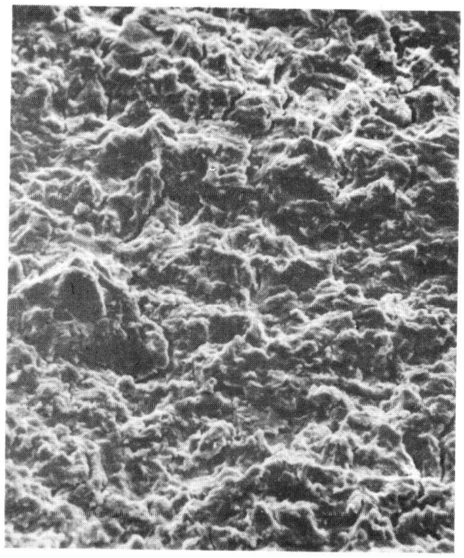

Fig. 5 Microfractograph of an adjusted CT specimen (500 × magnification)